Polymer 54 (2013) 4588–4593

Contents lists available at SciVerse ScienceDirect

Polymer

journal homepage: www.elsevier.com/locate/polymer

Unusual process-induced curl and shrinkage of electrospun PVDF membranes

B. Sundaray [a], F. Bossard [a,*], P. Latil [b], L. Orgéas [b], J.Y. Sanchez [c], J.C. Lepretre [c]

[a] Laboratoire Rhéologie et Procédés, UMR 5520, Université Joseph Fourier – CNRS – Grenoble INP, BP 53, 38041 Grenoble Cedex 9, France
[b] CNRS – Université de Grenoble (Université Joseph Fourier – Grenoble INP), Laboratoire Sols-Solides-Structures-Risques (3SR Lab, UMR 5521), BP 53, 38041 Grenoble Cedex 9, France
[c] LEPMI, Laboratoire d'Electrochimie et de Physicochimie des Matériaux et des Interfaces, UMR 5279, CNRS – Grenoble INP – Université de Savoie – Université Joseph Fourier, BP 75, 38402 Grenoble Cedex 9, France

ARTICLE INFO

Article history:
Received 23 November 2012
Received in revised form
26 April 2013
Accepted 22 May 2013
Available online 10 June 2013

Keywords:
Electrospinning
Poly(vinylidene fluoride)
Solvent evaporation

ABSTRACT

A significant shrinkage of about 17% of poly(vinyliedene fluoride) (PVDF) fibrous membranes processed by electrospinning is reported and analyzed for the first time in this article. Such shrinkage leads to a time dependent curl of the membrane, probed by image analysis and tensile test measurements. Crystalline structure of PVDF is analyzed through X-ray diffraction and FTIR analyses while solvent evaporation is monitored by weight lost measurements. The electrospinning process induces a crystal structure change of PVDF from non-polar α phase to polar β phase exhibiting piezoelectric properties. The curl was modeled taking into account the bimorph structure of the polymer membrane deposited onto the aluminum substrate with the electric field acting on the PVDF through the piezoelectric effect. Besides, just after the processing, the membranes exhibited a nearly 15% weight loss ascribed to the evaporation of the solvents entrapped within the solid fibrous membranes. The piezoelectricity of the β-phase together with solvent evaporation may be responsible for the observed contraction inducing the curl, the second mechanism of evaporation being predominant.

1. Introduction

Electrospinning is a simple and versatile method to produce ultra thin fibers from polymer solutions or melt [1–4]. In this process, a charged jet undergoes an intense elongation through electrostatic forces leading to a drastic narrowing of the polymer jet. Concurrently, the solvent usually evaporates during this stage, leaving a solid fiber after traveling an air path of few centimeters. The diameter of these fibers vary between 10 nm and 10 μm. Due to its high aspect ratio, electrospun fibers and their corresponding membranes are very attractive for a wide range of applications such as tissue engineering, military protective clothing, filter media, nanosenors, high performance batteries etc [5,6]. The extremely fast transition from solution to solid and the elongation involve intense non-linear process that supposes to govern the polymer structuration within the fiber. Recently, S. Tripatanasuwan et al. [7] have shown that a slow evaporation rate of water on PEO jet leads to increase the elongation of the jet that become thinner. Changes in crystalline state of nylon-6 and nylon-12 have been noticed by tuning the evaporation kinetic during the electrospinning [8]. The evaporation kinetic is also most likely at the origin of the observed porous nanofibers and flat ribbons in electrospinning [9,10]. Such extremely fast solidification is responsible for structural, physical and mechanical properties (tensile modulus, surface functionalization, porosity, etc.) of polymer fibers.

Poly(vinylidene fluoride) (PVDF) is one of the widely used polymer because of its remarkable chemical, electrical and mechanical properties. Because of its piezoelectric and ferroelectrics properties PVDF has been used for transducers, nonvolatile memory and energy storage [11–16]. PVDF is a semi-crystalline polymer with a complex structure. It can have four possible conformations namely α, β, γ and δ [16–20]. The α structure having TGTG form (in trans-gauche) is the dominant phase observed for PVDF. The δ form is the polar analog of the α phase while the β and γ phases have TTTT (planar zigzag) and GTTT conformations respectively. Among the four conformations, α is non-polar whereas β, γ and δ are polar, for which the β-phase has the largest spontaneous polarization per unit cell. Hence, the β-phase attracts technological interest, for its ferroelectrics, pyroelectric and piezoelectric properties. A lot of research effort has been invested in optimizing PVDF toward yielding materials with high β-phase content. This phase can be obtained from α or γ-phase by drawing and poling at high electric

* Corresponding author.
E-mail address: frederic.bossard@ujf-grenoble.fr (F. Bossard).

0032-3861/$ – see front matter © 2013 Elsevier Ltd. All rights reserved.
http://dx.doi.org/10.1016/j.polymer.2013.05.049

field. The conditions under which the β-phase can be induced depend strongly on the processing, thermal or mechanical treatments that the polymer undergoes [21–25]. Several authors investigated the optimal conditions for this conversion. Electrospinning is one of the methods where the PVDF converts to β-phase *in situ* [24,25].

In this article, the electrospinning process has been used to produce PVDF fibrous membranes and we report for the first time unusual shape changes of the so-formed membranes during and after their processing. Such shape changes, combining significant shrinkage and curl were observed and characterized during the first 2 h following the start of the electrospinning process up to 10 h after processing.

2. Experimental details

2.1. Materials

Poly(vinylidene fluoride) (PVDF) homopolymer Kynar 301F was obtained from Arkema in dry powder form. N,N dimethylformamide (DMF) and acetone were purchased from Sigma Aldrich. All the materials were used as received without further purification.

2.2. Methods and characterizations

Polymer solutions at the concentration of 17.7 wt% were prepared by dispersing PVDF in a mixture of DMF and acetone (40:60 v/v). The solutions were homogenized by heating at 80 °C with constant stirring for 2 h. Prior to process the solutions by electrospinning, the clear solutions of PVDF were cooled down to room temperature.

A homemade electrospinning setup was used to prepare PVDF fibers. It consists of a dual high voltage power supply (±30 kV, iseq GMBH Germany), a syringe pump (KDS Scientific model 200) and a fiber collector for the substrate, *i.e.* a rectangular aluminum foil. During electrospinning a constant flow rate of 0.02 ml min^{-1} was maintained with an electric potential difference of 12 kV between the electrodes. The relative humidity and the temperature of the electrospinning chamber were 45–50% HR and 30 °C, respectively. A D300 Nikon digital camera was used to capture the images at the interval of 15–20 min to observe qualitatively the curl and the contraction of PVDF membranes induced during the spinning process (see Fig. 4 and the supplementary movie 1). To better characterize the observed shape changes and their possible origins, the following methods and procedures were followed:

Supplementary video related to this article can be found at http://dx.doi.org/10.1016/j.polymer.2013.05.049.-(ii)

Supplementary video related to this article can be found at http://dx.doi.org/10.1016/j.polymer.2013.05.049.

- 1 h after the starting time t_0 of the electrospinning process, a square sample was cut from a processed membrane and the time evolution of its weight was recorded using a Mettler Toledo AG245 balance interfaced with a personal computer.
- 2 h after t_0, three rectangular slender strips were cut from the same membrane in order to analyze quantitatively both (i) the natural (stress free) membrane curl and contraction and (ii) the force required to restrain the contraction:
  (i) The two first strips were cut perpendicularly to quantify any possible in-plane anisotropy. They were fixed at one of their extremities to a support. Their natural curl and contraction was observed by positioning the Nikon digital camera perpendicular to the thickness of the strips (see Fig. 3(a) and supplementary movie 2). To analyze quantitatively the recorded shape changes, the centerlines of the strips were detected from the recorded 2D images using a standard skeletonization of the strips followed by a smoothing procedure of the resulting skeletons [26]. The in-plane contraction $\varepsilon_{contraction}$ of the strips could then be estimated from the initial l_{2h} and actual l curvilinear lengths of the centerlines, *i.e.* $\varepsilon_{contraction} = (l-l_{2h})/l_{2h}$. Besides, to analyze the curl of the strips after the first 2 h, some material points of the centerlines were also ascribed a local Frenet basis, allowing the calculation of the initial κ_{2h} and actual κ local curvatures of the strips. From the knowledge of the strip thickness e, current local maximal bending strain $\varepsilon_{bending}$ could then be estimated as $\varepsilon_{bending} = e|\kappa-\kappa_{2h}|/2$.
  (ii) The third strip was mounted into a micro-tensile testing machine equipped with a maximal load cell of 5 N. The strip was fixed into the tensile grips the positions of which were kept constant during the measurements. Then, the time evolution of the tensile force required to restrain the in-plane contraction of the tested strip was recorded.

After processing, membrane morphology was observed by scanning electron microscopy using Zeiss ultra 55 FESEM. A thin layer of platinum was sputtered onto the membranes before examination purposely. Besides, X-ray diffraction pattern of samples extracted from the initial PVDF powder and the processed membranes were recorded using PanAlytical X'pert Pro powder X-ray diffractometer using Cu Kα radiation (1.5406 A). Similarly, FTIR spectra were collected using a Perkin Elmer FTIR spectrometer. The samples were placed on top of the ATR set and scanned from 2000 to 650 cm^{-1}.

3. Results and discussion

3.1. Microstructures of the processed membranes

Fig. 1 shows FESEM micrographs of PVDF electrospun membranes at two different magnifications. The membranes network

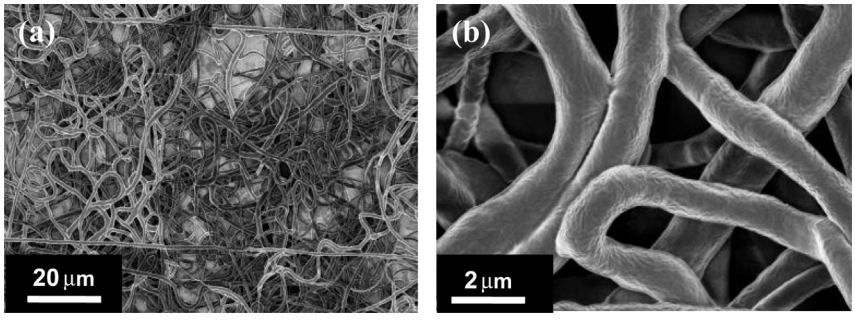

Fig. 1. FESEM images of PVDF electrospun fibers. (a) and (b) shows fibers collected on static collector or randomly oriented membrane at different magnification.

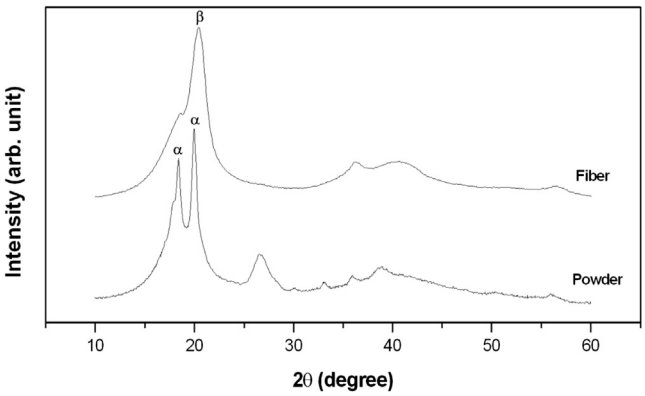

Fig. 2. X-ray diffraction of PVDF powder and nanofibrous mesh.

structure is highly porous (average porosity $\phi \approx 75\%$ measured by the Archimedes Method) with interconnected pores having an average diameter of 2–10 μm and with wavy fibers displaying planar random fiber orientation and fiber diameter ranging from 150 nm to 5 μm. It is interesting to notice that the fibers also exhibit rough surfaces.

Fig. 2 shows X-ray diffraction pattern of PVDF powder and electrospun membrane. The presence of peaks for the powder sample at $2\theta = 17.86°$, 20.1° and 26.8° which correspond respectively to the (100), (110) and (021) reflection planes, confirms that the initial PVDF powder are predominantly in the α-phase. In contrast, the electrospun membranes exhibit different peaks. In particular, the presence of peaks at $2\theta = 20.6°$ which correspond to the (110) and (200) planes confirms the presence of β-phase in the electrospun fibers [24,26].

In order to further check such a process-induced phase transformation, FTIR spectra of both the initial PVDF powder and the electrospun fibers were analyzed. Fig. 3 shows the presence of a unique absorption peaks for the powder at 762, 975 and 1383 cm^{-1}, confirming the presence of pure α-phase [27,28]. In case of electrospun fibers, the peaks recorded at 840 cm^{-1} (CH_2 rocking) and 1278 cm^{-1} (CF out-of-plane deformation) confirms the presence of β-phase in the electrospun fibers [29]. Therefore, it is established from the X-Ray diffraction and FTIR spectroscopy that some of initial PVDF powder which is mainly in the α-phase converts to β conformation during the electrospinning process. The conversion from non-polar α-phase to piezoelectric β-phase may be due to large elongational strains induced by high electrostatic potential

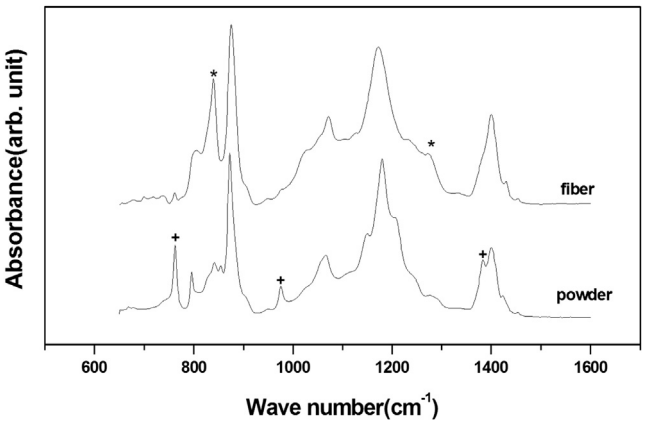

Fig. 3. FTIR spectra of PVDF powder and electrospun nanofiber membrane. The peaks correspond to α phase are marked as + and peaks correspond to β phase are marked as * symbol.

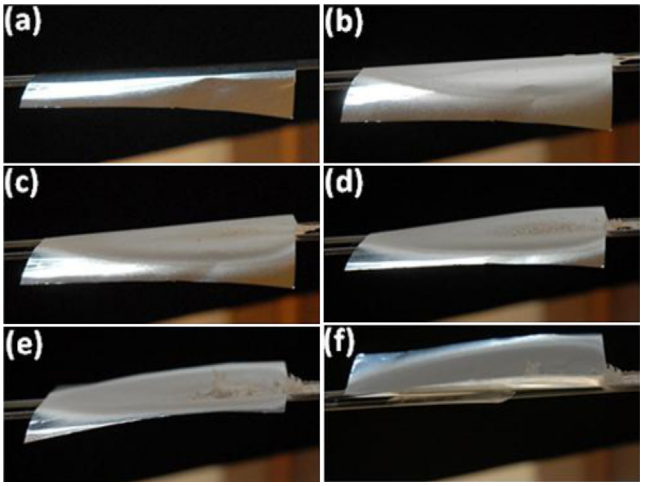

Fig. 4. Photographs (a), (b), (c), (d),(e) and (f) showing contractions of electrospun membranes taken at different time intervals during the electrospinning process. A video of the process is attached in the electronics version of the article.

applied during the electrospinning process, leading to fewer defects and smaller domain wall motion barrier in the nanofibers [24].

3.2. Shape changes of the membranes during processing

The macroscopic curl and contraction of the PVDF membrane during processing is pointed out in Fig. 4, showing photographs of the aluminum substrate with electrospun membranes collected at different time steps (the video of the process is available in the supporting document). Fig. 4(a) shows the image of the flat substrate at the beginning of the process, *i.e.* without fibers. The gradual change of the color of the substrate indicates the progressive deposition of fibers onto the surface as the collecting time increased. After nearly 20 min from the start of the experiment, the aluminum foil together with the PVDF membrane started to curl, as shown in Fig. 4(b). As the time progressed, more and more fibers were collected and the curl of the substrate and the membrane was enhanced, as emphasized in Fig. 4(b–e). Thereafter, the adhesion of the membrane on the aluminum foil was progressively lost, finally leading to a substantial isotropic in-plane shrinkage of the membrane of nearly 11% after the first 2 h.

One of the possible origins of (i) the curl and (ii) the shrinkage highlighted during the processing could be related to the piezoelectricity of the PVDF membrane and to the driving electrical field applied onto the electrospun membrane perpendicular to them (e_3 direction, see Fig. 5):

- In case (i), as the PVDF membrane was stuck onto the aluminum substrate, its in-plane shrinkage was restrained leading to internal

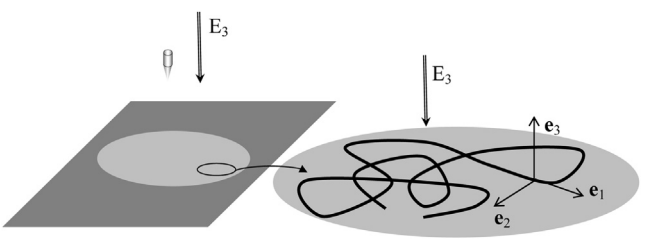

Fig. 5. Schematic of bimorph of Al foil and PVDF electrospun membrane with knife edge clamping configuration. The bimorph is in the *xy*-plane and the electric field (E_3) is along the *z*-direction. (b) Magnified graphic shows the *x*, *y* and *z* components of the piezoelectric coefficients.

in-plane contraction stresses. Thus, the "membrane + substrate" system could behave as a piezoelectric bimorph with one active element (*i.e.* the piezoelectric PVDF membrane) and one passive element (*i.e.* the aluminum substrate).

Assuming a strong influence of the piezoelectric effect induced by the electric field, the bimorph could bend, as observed in Fig. 4, with a maximal out-of-plane piezoelectric deflection of which the the magnitude Δl_{piezo} can be estimated as [32,33]:

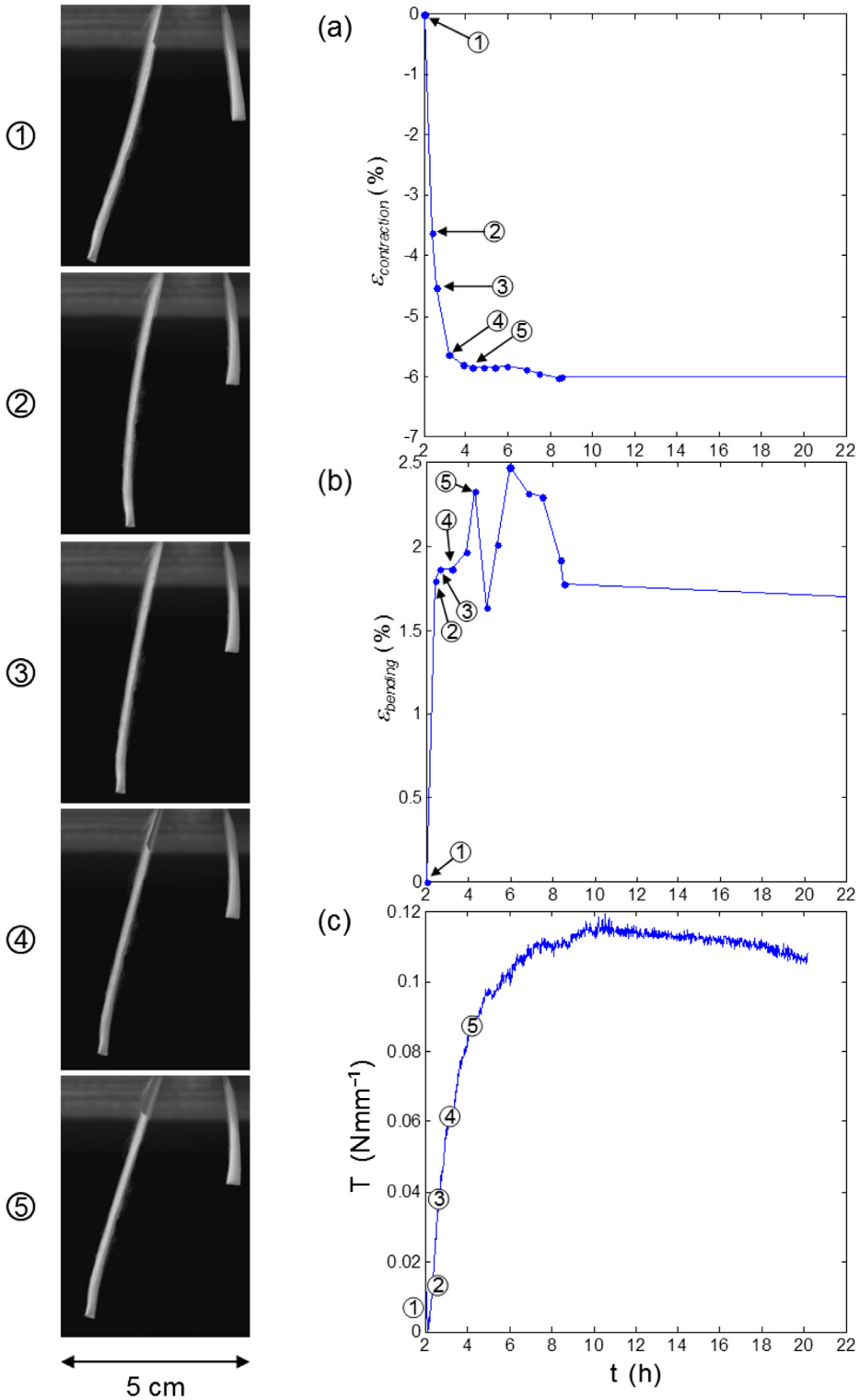

Fig. 6. 2D pictures (① to ⑤) taken at various time $t > t_0 + 2$ h and showing qualitatively the curl and the contraction of the two slender stress free strips. Graph (a): time evolution of the contraction $\varepsilon_{contraction}$ of centerlines of the two strips. Graph (b): time evolution of their maximal bending strain $\varepsilon_{bendingmax}$. Graph (c): time evolution of the tension T required to restrain the contraction of the third strip.

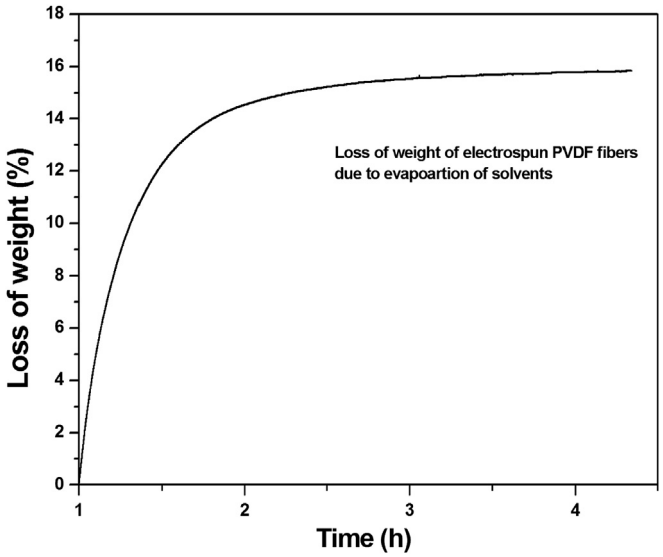

Fig. 7. Weight loss of the electrospun membrane with time due to evaporation of remaining solvent.

$$\Delta l_{\text{piezo}} = \left|\left(\frac{L}{2h}\right)^2 d_{31} V \frac{3kr(1+r)}{1+k^2r^4+2k(2r+3r^2+2r^3)}\right|$$

where L is the in-plane length of the bimorph ($\approx$100 mm), $r = h'/h$, h and h' being respectively the membrane and substrate thicknesses (a typical value $r \approx 1$ can be used in our case), d_{31} is the piezoelectric coefficient of the PVDF perpendicular to the electric field ($\approx$15 pm V^{-1} [30,31]), V is the voltage used during the processing and k is the ratio of the in-plane Young moduli of the aluminum substrate E_{Al} (=70 GPa) and the polymer membrane E_{m}. Accounting for the Young modulus E_{PDVF} of dense PVDF ($\approx$2.5 GPa) and assuming a planar random fiber orientation within the PVDF membrane, a reasonable estimation of E_{m} is $(1-\phi)\ E_{\text{PVDF}}/3 \approx 200$ MPa [34], so that $k \approx 350$. Thus, a rough estimate of the magnitude of the maximal out-of-plane deflection induced during the processing by piezoelectric effects should be $\Delta l \approx 0.12$ mm: it is one to two orders of magnitude lower than the deflection Δl_{exp} recorded during the membrane processing, as emphasized in Fig. 4 ($\Delta l \approx 10$–20 mm).

- In case (ii), when the adhesion of the membrane with its substrate is lost, the electric field applied during the processing could also induce a free-stress in-plane strain of magnitude $\varepsilon_{\text{piezo}} = |d_{31}E| \approx 10^{-4}$%: this strain magnitude is much below the 11% in-plane strain magnitude observed experimentally during the membrane shrinkage.

Hence, if the piezoelectricity could induce curl and in-plane shape change of the PVDF membrane during its processing, it is not the major phenomenon responsible of the large shape changes observed experimentally.

3.3. Shape changes of the membrane after processing

The time evolution of the in-plane membrane contraction $\varepsilon_{\text{contraction}}$ observed after the first 2 h is illustrated in Fig. 6(a) (the contractions of the two tested strips were found to be very similar and were then averaged in this figure).

As revealed from this figure, $\varepsilon_{\text{contraction}}$ rapidly decreased down to -6% and remained nearly constant after 10 h. Such a contraction is accompanied with a noteworthy curl of the strips, as emphasized from both the pictures shown in Fig. 6 and the graph plotted in Fig. 6(b): the time evolution of the maximal bending strain $\varepsilon_{\text{bendingmax}} = \max(\varepsilon_{\text{bending}})$ follows a trend similar to $\varepsilon_{\text{contraction}}$, *i.e.* a fast increase up to a constant plateau of about 2%. Besides, as shown in Fig. 6(c), when restrained, shrinkage micro-mechanisms induced a significant reacting tension T, defined as the ratio of tensile force by the strip width, which rapidly increased up to about 0.11 N mm^{-1} during the first 10 h and remained approximately constant afterwards.

Fig. 7 shows weight loss of the electrospun membrane (1 h from the start t_0 of electrospinning process) with time: a nearly 15.6% loss of weight is observed between $t_0 + 1$ h and $t_0 + 2$ h.

Such a considerable weight loss is ascribed to the evaporation of the solvents remaining within the fibrous membrane during and after the electrospinning process. This unusual and delayed solvent evaporation is presumably induced (i) by the possible heterogeneous nanostructure of the fibers and (ii) by the probable presence of DMF, the boiling temperature of which being rather high (153 °C). The presence of remaining DMF solvent can explain that fibers are interconnected after deposition on the collecting substrate. Indeed, polymer fibers are soft enough to locally merge at their contact points.

The observed evaporation may be responsible of the very rough surface of the processed fibers (see Fig. 1). Evaporation-induced surface contraction is the driving effect leading to the formation of polymer fibers during the electrospinning. This effect has been modeled in the jet [35] but has never been observed in the fibers. However, solvent evaporation is likely to induce a severe contraction of the PVDF fibers in their solid state. This microscale contraction should in turn induce the various macroscale shape changes highlighted during and after the electrospinning (see Figs. 4 and 6):

- When the membrane sticks onto its aluminum substrate (*i.e.* during the electrospinning), such a local contraction is more or less constrained. Under such circumstances, the PDVF membrane is able to develop significant shrinkage stresses, as emphasized from Fig. 6(c), and thus to induce the macroscale curl of the bimorph PVDF + Al (see Fig. 4).
- When the adhesion of the membrane to the aluminum substrate is lost (*i.e.* during or after processing), the local fiber

contraction can freely occur up to the end of the evaporation process. Thereby, the membrane freely shrinks, as evident from Fig. 6(a). It also freely curls (see Fig. 6(b)), this phenomenon being ascribed both to the possible heterogeneity of the fibrous architecture and the different evaporation kinetic through the membrane thickness.

Such contraction of electrospun membranes induced by delayed evaporation of solvent within the fibers could be harmful for many applications and consequently has to be reduced. Recently, Na et al. [36] have shown that an increase of the evaporation kinetic leads to produce more homogeneous fibers by reducing the size distribution. Consequently, solvent evaporation kinetics have to be speed up during the process. For this purpose, low boiling point solvent as well as high temperature processing and, in a certain extent, low pressure environment can be preferred.

4. Conclusion

Nano-fibrous PVDF membranes exhibiting piezoelectric β-phase were successfully electrospun. However, during processing substantial, unusual and undesirable curl and contraction of the membranes were observed. These shape changes were characterized and were ascribed both to the reverse piezoelectric effect under high electrostatic field and delayed solvent evaporation. The first phenomenon is active only during the processing phase and its influence on the observed shape changes is minor. On the contrary, the solvent evaporation is presumably the main driving mechanisms that will be analyzed more closely in future works.

Acknowledgments

This work has been performed with the financial support of Grenoble Institut National Polytechnique. The authors gratefully acknowledge R. Martin from the Laboratoire CMTC for providing the SEM observations. P. Latil gratefully acknowledges the French National Research Agency (ANR) for its research grant (ANAFIB, ANR-09-JCJC-0030-01).

References

[1] Formhals A. US Patent No. 1,975,504; 1934.
[2] Doshi J, Reneker DH. J Electrostat 1995;35:151–60.
[3] Fridrikh SV, Yu JH, Brenner MP, Rutledge GC. Phys Rev Lett 2003;90:144502.
[4] Tan SH, Inai R, Kotaki M, Ramakrishna S. Polymer 2005;46:6128–34.
[5] Sridhar R, Venugopal JR, Sundarrajan S, Ravichandran R, Ramalingam B, Ramakrishna S. J Drug Deliv Sci Technol 2011;21:451–68.
[6] Dong Z, Kennedy SJ, Wu Y. J Power Sources 2011;196:4886–904.
[7] Giller CB, Chase DB, Rabolt JF, Snively CM. Polymer 2010;51:4225–30.
[8] Tripatanasuwan S, Zhong Z, Reneker DH. Polymer 2007;48:5742–6.
[9] Koombhongse S, Liu W, Reneker DH. J Polym Sci Part B Polym Phys 2001;39:2598–606.
[10] Bognitzki M, Czado W, Frese T, Schaper A, Hellwig M, Steinhart M, et al. Adv Mater 2001;13:70–2.
[11] Nalwa HS. Ferroelectric polymers: chemistry, physics, and applications. New York: Dekker; 1995.
[12] Naber RCG, Asadi K, Blom PWM, de Leeuw DM, de Boer B. Adv Mater 2010;22:933–45.
[13] Guan F, Wang J, Pan J, Wang Q, Zhu L. Macromolecules 2010;43:6739–48.
[14] Wu N, Cao Q, Wang X, Li X, Deng H. J Power Sources 2011;196:8638–43.
[15] Choi SW, Kim JR, Ahn YR, Jo SM, Cairns EJ. Chem Mater 2007;19:104–15.
[16] Tashiro K. Crystal structure and phase transition of PVDF and related copolymers. In: Nalwa Hari Singh, editor. Ferroelectric polymers (chemistry, physics, and applications), 63. New York: Marcel Dekker; 1995.
[17] Hasegawa R, Takahashi Y, Chatani Y, Tadokoro H. Polym J 1972;3:600–10.
[18] Lovinger AJ. J Polym Sci Polym Phys Ed 1980;18:793–809.
[19] Lovinger AJ. Science 1983;220:1115–21.
[20] Mohajir B, Heymans N. Polymer 2001;42:5661–7.
[21] Li J, Meng Q, Li W, Zhang Z. J Appl Polym Sci 2011;122:1659–68.
[22] Kobyashi M, Tashiro K, Tadokoro H. Macromolecules 1975;8:158–71.
[23] Davis GT, McKinney JE, Broadhurst MG, Roth SC. J Appl Phys 1978;49:4998–5002.
[24] Yee WA, Kotaki M, Liu Y, Lu X. Polymer 2007;48:512–21.
[25] Pu J, Yan X, Jiang Y, Chang C, Lin L. Sensors Actuators A Phys 2010;164:131–6.
[26] Latil P, Orgéas L, Geindreau C, Dumont PJJ, Roscoat SR. Compos Sci Technol 2011;71:480–8.
[27] Bachmann MA, Gordon WL, Koenig JL, Lando JB. J Appl Phys 1979;50:6106–12.
[28] Lanceros-Mendez S, Mano JF, Costa AM, Schimdt VH. J Macromol Sci Phys B 2001;40:517–27.
[29] Bormashenko Y, Pogreb R, Stanevsky O, Bormashenko E. Polym Test 2004;23:791–6.
[30] Mellinger A. IEEE Trans Dielectr Electr Insul 2003;10:842–61.
[31] Kepler RG, Anderson RA. J Appl Phys 1978;49:4490–4.
[32] Kholkin AL, Wutchrich C, Taylor DV, Setter N. Rev Sci Instrum 1996;67:1935–41.
[33] Steel MR, Harrison F, Harper PG. J Phys D Appl Phys 1978;11:979–89.
[34] Perkins RW, Mark RE. In: Bradler J, editor. The role of fundamental research in paper making, vol. 1. London: Mech. Eng. Publ.; 1983. p. 479–526.
[35] Wu X-F, Salkovskiy Y, Dzenis YA. App Phys Lett 2011;98:223108.
[36] Na H, Liu X, Sun H, Zhao Y, Zhao C, Yuan X. J Polym Sci Part B Polym Phys 2010;48:372–80.